Comparative Finite Element Analysis of Osseointegration System in Trans-Radial Amputation: A Proposal of New Design

Seung Gun Lee
Hanyang University Seoul Hospital
Heaseong Jeoung
Hanyang University
Dong-Hong Kim
Hanyang University Seoul Hospital
Chang-Hun Lee (drlch79@hanyang.ac.kr)
Hanyang University Seoul Hospital

Research Article

Keywords: Finite element analysis, Trans-radial amputation, Osseointegration

Posted Date: December 28th, 2020

DOI: https://doi.org/10.21203/rs.3.rs-128848/v1

Abstract

Introduction: Conventional osseointegration systems have been applied in patients requiring trans-humeral and trans-femoral amputations. However, the application of these systems to trans-radial amputations is limited by the small diameter of the radius and ulna. Our study aimed to compare the biomechanical stability of a novel osseointegration system with that of a conventional system used in trans-radial amputations using a finite element(FE) models.

Methods: We established three-dimensional FE models of trans-radial amputations, which were osseointegrated with both the novel and conventional systems. External loads were applied to the FE models with compressive force and tensile force along the long axis, horizontal shear force, and vertical shear force. The maximum equivalent stress(MES) and the distribution of stress through the radius and ulna was evaluated.

Results : The MES of the radius and ulna was higher in the conventional system when compressive, tensile, and vertical shear forces were applied. However, when the horizontal shear force was applied, the opposite result was found. The distribution of stress was more effective in the novel system.

Conclusion : Three-dimensional FE modeling showed that the novel system enables to have a lower stress level and a more even distribution of stress for osseointegration in trans-radial amputations.

Introduction

Trans-radial amputation may result from a congenital condition, trauma, infection or tumor.[1] In the cases of upper extremity amputations, trauma is the leading cause, accounting for 80% of acquired amputations and occurring most often in men aged 15 to 45 years. Meanwhile, the second most prevalent cause is tumor and vascular complications of diseases.[2] The prevalence of amputations was 1.6 million in 2005, with projections suggesting this prevalence may double by the year 2050.[3]

The upper extremities are highly complex limbs with neurovascular bundles, lymphatics, muscles, and bones that come together to form a functional appendage used during daily activities.[2] As such, the loss of the wrist and/or hand leads to functional and psychological problems. Depending upon the level of amputation, various clinical considerations exist; ultimately, the goal in any amputation is to save all viable tissue as this directly correlates with improved functional status.[4,5] Lee et al[6] reported that close proximity of the amputation site to the elbow significantly decreased residual function, including forearm rotational movement. Therefore, it is important to preserve the length of the radius as much as possible.

Currently, only a few osseointegrated transcutaneous prosthetic systems(such as OPRA system, Integrum AB from Mölndal, Sweden and ITAP from Stanmore Medical Group, Stevenage, England) for use in humans exist but none are approved for general use in the United States.[7,8] Conventional osseointegration systems have been applied to trans-humeral(OPRA system and ITAP system) and trans-femoral amputations(OPRA system and ISP Endo/Exo prosthesis from ESKA Implants AG, Lubeck,

Germany). However, the application of these systems in patients requiring trans-radial amputations have limitations due to the small diameter of the radius and ulna. The average intramedullary canal diameter of the humerus is 14.5 mm(range : 9.4 ~ 20.5 mm)[9], while the average diameter of the medullary cavity of the distal shaft of the radius is 6.7 mm(range : 6.1 ~ 7.3 mm) and the minimum diameter of the ulna medullary cavity is 4.2 mm(range : 2 ~ 6.7 mm).[10,11]

In a review of the literature, no biomechanical study about osseointegrated implants for the trans-radial amputee was found. Because major upper-extremity amputees account for only 8% of the 1.5 million individuals living with limb loss[3] and upper-extremity loss does not affect weight-bearing,[11] therefore, the importance of upper-extremity amputation is lowered. In addition, it is important to recover the fine-movement capacity of the upper extremity, especially the hand and wrist, so it is considered to be because the difficulty is higher than that of the lower-extremity reconstruction. Applying a small implant with the same design as the conventional system can increase the risk of periprosthetic fracture due to stress concentration in the forearm bone. Through these points, the need for a new design for osseointegration in the forearm bones has emerged.

From these points, we made a new design implant with several modification. And in a similar way to Kaku et al, our study aimed to evaluate the stress-distribution pattern and biomechanical stability of a novel osseointegration system and to compare it with that of the conventional system in trans-radial amputation using a finite element(FE) model. We hypothesized that the novel system will reduce the stress intensity and more evenly distribute stress loading throughout the radius and ulna.

Results

When a loading force of 60N was applied on the implant along the Y-axis(vertical shear force) and the Z-axis(compressive and tensile force), the maximum equivalent stress was higher in the conventional model rather than in the novel model except for in Sect. 3 of the ulna. However, when a horizontal shear force of 60N was applied(X-axis), the novel system received more stress than the conventional system in Sect. 2 and 3 of the radius and Sect. 1 and 2 of the ulna(Table 2).

The stress at the proximal radius and ulnar shaft was decreased in the novel system when stress was loaded along the X-axis(horizontal shear), while that at the shaft of the radius was increased in the novel system condition(Fig. 3). When stress was loaded along the Y-axis(vertical shear force), the stress concentration throughout the radius was decreased in the novel system(Fig. 4). Finally, when stress was applied along the Z-axis(compressive and tensile forces), the stress concentration throughout the radius and ulna was decreased in the novel system(Fig. 5).

Discussion

Patients with amputated limbs have traditionally relied on a stump-socket interface for prosthetic attachment.[7] This type of prosthetic design is associated with several problems, such as skin changes,

increased energy expenditure during ambulation, and disuse osteopenia.[12–14] Several types of osseointegration systems have been developed to overcome these problems and are currently clinically available; however, these osseointegration systems also encountered several problems of their own, which are infection, periprosthetic bone fracture, bone loss due to stress shielding, and implant failure.[15,16] Furthermore, we are concerned that the conventional design available for trans-humeral and trans-femoral amputees is not suitable for the trans-radial amputee. Specifically, the short length of the conventional system inserted into a long bone with a small diameter increases the risk of periprosthetic fracture due to targeted stress concentration.

Osseointegrated implants are exposed to daily activities, consisting of flexion, extension, supination, and pronation of the elbow and radial deviation and ulnar deviation of the wrist. Our study showed that, when subjected to horizontal shear force, the radius and ulna received higher maximum equivalent stress in the novel system. In contrast, with compressive, tensile, and vertical shear forces, the radius and ulna received lower maximum equivalent stress in the novel system. Thus, more even stress distribution throughout the radius and ulna was observed in the novel system. The stress loaded along the X-axis(horizontal shear force) is assumed to be that loaded during radial and ulna deviation of the wrist, while the stress loaded along the Y-axis(vertical shear force) is assumed to be the force loaded during flexion and extension of the elbow and wrist. Compressive and tensile forces along the Z-axis are assumed to be the result of longitudinal movements characterized by changes in ulnar variance relative to the radial corner during forearm supination and pronation.

The novel system has a long stem, sharing the characteristic of an intramedullary nail. Osseointegration through the whole length of the radius and ulna was supposed to evenly distribute stress transferred from the distal end of the implants. Ding et al[17] reported that increasing the diameter and length of the implant decreased the stress and strain on the alveolar crest per biomechanical analysis of high-quality FE models of complete range mandibles. Baggi et al[18] also reported the influence of implant diameter and length on the stress distribution of osseointegrated implants related to crestal bone geometry. Stress values and concentration areas are decreased for cortical bone when the implant diameter is increased, whereas more effective stress distributions for cancellous bone were observed with increasing implant length.[18] In the case of trans-radial amputation, the medullary diameter of the radius and ulna is not a modifiable factor, but the length of the implant is. The results of our study were consistent with those of previous studies in that the implant length affected the stress distribution and maximum equivalent stress.

Despite our good results, two problems of the novel system were recognized during FE analysis. First, the maximum equivalent stress of the radius and ulna in the horizontal shear force was higher in the novel system. Also, the stress distribution in Sect. 3 of the ulna in the novel system was definitely less effective than that seen with the conventional system. Notably, the radius can experience physiologic bowing in the horizontal plane[19] and adaptation to this physiologic bowing by deep insertion of the long stem seems to be the cause of greater maximum equivalent stress. In the implant design, the diameter of shaft

of the novel radial implant was 3.0 mm(supplement). To decrease the stress value in relation to horizontal force, a larger radial-implant diameter can be considered. Also, increased stress around the distal longitudinal grooves of both the radius and ulna implants was observed. There is a tendency to increase the stress value in the angled location rather than the cylindrical or smooth location in FE analysis. According to Xiaobin et al[20], when the surfaces are angled, the stress concentration is large when forces are applied from multiple directions. Conversely, when the surfaces were rounded, it was found that the stress concentration was relatively low for the same external forces. For clinical application of the implants, a cylindrical design rather than an angular groove modality might reduce bone absorption in the insert area.

Stenlund et al[21] found that the elastic strains and principal compressive stresses in the bone in direct contact with the abutment at the most distal location may indicate unfavorable bone remodeling, resulting in a decrease in bone density with time. Meanwhile, Nebergall[15] et al reported that the transmission of loads to the contact point between the bone and implant can cause cortical thinning or bone resorption. This results a high risk of loosening of that area, together with various complications in the distal portion, including implant loosening and periprosthetic fractures. Ultimately, the need for reoperation to replace the entire implant will increase.[22]

Our study has some limitations. First, there was a lack of simulation of the anisotropic material properties of human bone. Although the FE model was designed by distinguishing the material properties of cortical and cancellous bone, this does not fully reflect the material properties of human bone. Moreover, the amputated site may present a combination of damaged bone, callus, hematoma, and fibrotic tissues. Additional analysis is likely required in future research, incorporating detailed simulation of a more realistic bone model and some clinical cases. Second, it should be realized that this loading configuration does not represent a whole trans-radial amputation case. When applied in clinical practice, amputation levels and the loss of soft tissue including muscles vary between patients. Thus, these findings should be generalized with caution. Despite these limitations, however, we investigated the biomechanical properties of the novel and conventional implants for the trans-radial amputee and confirmed the chance of improvement of osseointegration in the forearm bone.

In conclusion, three-dimensional FE models showed that the design of a novel system provides a lower stress level and more even stress distribution for osseointegration in trans-radial amputation. This novel osseointegration system is expected to reduce complications such as periprosthetic fracture and implant failure and to improve long-term implant survival.

Material And Methods

FE modeling

We established three-dimensional FE models of trans-radial amputations, which were osseointegrated with novel and conventional systems. We used the Ansys Workbench version 17.0 software

program(Ansys Inc., Canonsburg, PA, USA) to create FE models. Two FE models were created, one representing a trans-radial amputation with a conventional osseointegration implant and the other representing the same forearm bones with a novel osseointegration implant. The geometry of the forearm bones was acquired from computed tomography scans(slice thickness : 1mm) of a 34-year-old male patient's forearm bones. The main cause of trans-radial amputation is trauma(up to 80%), which occurs in young men(aged 15 ~ 45 years),[2] so we set the FE model to incorporate the normal bone mineral density of a typical young man. This study was approve by our institutional review board(HYUH-2020-07-017) and we obtained informed consent from the patient.

The amputated radius and ulna model represented the most functional osteotomy level of 18cm below the olecranon tip.[6] The surface-shape contours of the two implants were fitted in both forearm bones and implemented into the FE models. In this process, we designed the FE model under two conditions. First, the implants with the same outer diameter of the intermedullary part were assumed to be in close contact with the bone. Second, the implant and bone were bonded to represent full osseointegration.

Material properties

The FE model was fixed at the end of the amputation level of the radius and ulna and the interface between the implant and bone was modeled as a continuous bond. This arrangement implies ideal osseointegration was achieved without any relative motion at the interface. In other words, the implant was rigidly anchored in the bone, showing a fixed and similar type of bond at all prosthesis material interfaces. The biomechanical properties of the radius and ulna bones were composed of cortical bone and cancellous bone. The setting values are described in Table 1.

Loading conditions and measurements

External loads were applied to the FE models with compressive and tensile forces measuring 60N along the long axis(Z-axis). Horizontal shear force(X-axis) and vertical shear force(Y-axis) to the FE models were similarly applied at a strength of 60N. Horizontal shear force is a force assuming a stress situation that occurs when radial and ulnar deviation movements occur in the wrist. Vertical shear force is a force assuming a stress situation that occurs during flexion and extension movements in the wrist and elbow. The maximum equivalent stress around integrated implants in the radius and ulna was calculated. Also, the stress-distribution pattern of the load applied to the whole length of the radius and ulna was evaluated in three sections(Figure 1). All experiments were performed in accordance with relevant named guidelines and regulations.

Implant design

Currently, there is no conventional osseointegration system available for trans-radial amputees. Therefore, a conventional osseointegration system was modeled after the shape of a trans-humeral or trans-femoral implant, which has already been applied in clinical cases. A new implant was designed by modifying several points in the conventional osseointegration system(Figure 2); specifically, we designed

to allow proximal screw fixation to achieve initial rotational stability in the novel osseointegration system. The surface of the implant was treated with a porous coating so that bony ingrowth could occur better in the distal part of the implant, while a longitudinal groove was devised to increase the contact area. In addition, the radius and ulna have a slight curvature(bowing); so, to reduce the occurrence of iatrogenic damage such as cortical breakage or fracture. And the diameter of the implant's middle area was designed smaller so as to be more easily bent, facilitating greater adaptation during the implant-insertion process. Finally, the stem was designed to be longer to reduce the stress concentration at the proximal end of the integrated implant and to distribute the stress more broadly throughout the radius and ulna.

Declarations

Acknowledgement

This work was supported by the National Research Foundation of Korea(NRF) grant funded by the Korea government(MSIT)(No. 2020R1A2C2101353) and the research fund of Hanyang University (HY-2020).

Author contributions

This paper was written with S.G. Lee and H. Jeoung performing equally as the first authors. D.H. Kim was in charge of data analysis and summarization. All of this study was performed under C.H. Lee's supervision.

Additional Information

Competing interests

The authors declare no competing interests.

References

1. Amornvit, P., Rokaya, D., Keawcharoen, K. & Thongpulsawasdi, N. Stress distribution in implant retained finger prosthesis: a finite element study. *J Clin Diagn Res* **7**, 2851–2854, doi:10.7860/JCDR/2013/7001.3775 (2013).
2. Maduri, P. & Akhondi, H. in *StatPearls* (2020).
3. Ziegler-Graham, K., MacKenzie, E. J., Ephraim, P. L., Travison, T. G. & Brookmeyer, R. Estimating the prevalence of limb loss in the United States: 2005 to 2050. *Arch Phys Med Rehabil* **89**, 422–429, doi:10.1016/j.apmr.2007.11.005 (2008).
4. Atroshi, I. & Rosberg, H. E. Epidemiology of amputations and severe injuries of the hand. *Hand Clin* **17**, 343–350, vii (2001).
5. Dillingham, T. R., Pezzin, L. E. & MacKenzie, E. J. Limb amputation and limb deficiency: epidemiology and recent trends in the United States. *South Med J* **95**, 875–883, doi:10.1097/00007611-200208000-00018 (2002).

6. Lee, G. *et al.* Residual rotation of forearm amputation: cadaveric study. *BMC Musculoskelet Disord* **21**, 40, doi:10.1186/s12891-020-3050-x (2020).
7. Grisez, B. T., Hanselman, A. E., Boukhemis, K. W., Lalli, T. A. J. & Lindsey, B. A. Osseointegrated Transcutaneous Device for Amputees: A Pilot Large Animal Model. *Adv Orthop* 2018, 4625967, doi:10.1155/2018/4625967 (2018).
8. Tomaszewski, P. K., van Diest, M., Bulstra, S. K., Verdonschot, N. & Verkerke, G. J. Numerical analysis of an osseointegrated prosthesis fixation with reduced bone failure risk and periprosthetic bone loss. *J Biomech* **45**, 1875–1880, doi:10.1016/j.jbiomech.2012.05.032 (2012).
9. Barth, J. *et al.* Is global humeral head offset related to intramedullary canal width? A computer tomography morphometric study. *J Exp Orthop* **5**, 35, doi:10.1186/s40634-018-0148-2 (2018).
10. Kaku, N., Tanaka, A., Tagomori, H. & Tsumura, H. Finite Element Analysis of Stress Distribution in Flat and Elevated-Rim Polyethylene Acetabular Liners. *Clin Orthop Surg* **12**, 291–297, doi:10.4055/cios19145 (2020).
11. Pierrie, S. N., Gaston, R. G. & Loeffler, B. J. Current Concepts in Upper-Extremity Amputation. *J Hand Surg Am* **43**, 657–667, doi:10.1016/j.jhsa.2018.03.053 (2018).
12. Dudek, N. L., Marks, M. B., Marshall, S. C. & Chardon, J. P. Dermatologic conditions associated with use of a lower-extremity prosthesis. *Arch Phys Med Rehabil* **86**, 659–663, doi:10.1016/j.apmr.2004.09.003 (2005).
13. Meulenbelt, H. E., Geertzen, J. H., Jonkman, M. F. & Dijkstra, P. U. Skin problems of the stump in lower limb amputees: 1. A clinical study. *Acta Derm Venereol* **91**, 173–177, doi:10.2340/00015555-1040 (2011).
14. Waters, R. L. & Mulroy, S. The energy expenditure of normal and pathologic gait. *Gait Posture* **9**, 207–231, doi:10.1016/s0966-6362(99)00009-0 (1999).
15. Nebergall, A. *et al.* Stable fixation of an osseointegated implant system for above-the-knee amputees: titel RSA and radiographic evaluation of migration and bone remodeling in 55 cases. *Acta Orthop* **83**, 121–128, doi:10.3109/17453674.2012.678799 (2012).
16. Tillander, J., Hagberg, K., Hagberg, L. & Branemark, R. Osseointegrated titanium implants for limb prostheses attachments: infectious complications. *Clin Orthop Relat Res* **468**, 2781–2788, doi:10.1007/s11999-010-1370-0 (2010).
17. Ding, X., Liao, S. H., Zhu, X. H., Zhang, X. H. & Zhang, L. Effect of diameter and length on stress distribution of the alveolar crest around immediate loading implants. *Clin Implant Dent Relat Res* **11**, 279–287, doi:10.1111/j.1708-8208.2008.00124.x (2009).
18. Baggi, L., Cappelloni, I., Di Girolamo, M., Maceri, F. & Vairo, G. The influence of implant diameter and length on stress distribution of osseointegrated implants related to crestal bone geometry: a three-dimensional finite element analysis. *J Prosthet Dent* **100**, 422–431, doi:10.1016/S0022-3913(08)60259-0 (2008).
19. Firl, M. & Wunsch, L. Measurement of bowing of the radius. *J Bone Joint Surg Br* **86**, 1047–1049, doi:10.1302/0301-620x.86b7.14294 (2004).

20. Xiaobin Le, P. E. & Zelong, L. (ASEE Conferences, Atlanta, Georgia, 2013).
21. Stenlund, P. *et al.* Effect of load on the bone around bone-anchored amputation prostheses. *J Orthop Res* **35**, 1113–1122, doi:10.1002/jor.23352 (2017).
22. Al Muderis, M., Khemka, A., Lord, S. J., Van de Meent, H. & Frolke, J. P. Safety of Osseointegrated Implants for Transfemoral Amputees: A Two-Center Prospective Cohort Study. *J Bone Joint Surg Am* **98**, 900–909, doi:10.2106/JBJS.15.00808 (2016).

Tables

Table 1. Bone material property values

	Cortical bone		Cancellous bone	
Material properties	Value	Unit	Value	Unit
Young's modulus X direction	6,900	MPa	680	MPa
Young's modulus Y direction	8,500	MPa	1,210	MPa
Young's modulus Z direction	18,400	MPa	2,050	MPa
Poisson's ratio XY	0.42	-	0.14	-
Poisson's ratio YZ	0.31	-	0.1	-
Poisson's ratio XZ	0.32	-	0.11	-
Shear modulus XY	2,400	MPa	330	MPa
Shear modulus YZ	4,900	MPa	600	MPa
Shear modulus XZ	3,600	MPa	400	MPa

Table 2. Maximum equivalent stress at each section after an external load(60N) applied along each axis.

(A) External load(60N) application along the X-axis

		Section 1	Section 2	Section 3
Conventional system	Radius	29.123	32.484	13.027
	Ulna	39.335	22.351	17.008
Novel system	Radius	24.194	42.453	14.63
	Ulna	104.09	28.816	16.03

(B) External load(60N) application along the Y-axis

		Section 1	Section 2	Section 3
Conventional system	Radius	52.21	31.281	27.361
	Ulna	15.329	23.733	21.674
Novel system	Radius	49.414	30.366	25.523
	Ulna	14.38	22.581	57.157

(C) External load(60N) application along the Z-axis

		Section 1	Section 2	Section 3
Conventional system	Radius	1.3949	1.9997	1.1668
	Ulna	1.1521	1.1741	3.0583
Novel system	Radius	0.95711	1.593	0.76815
	Ulna	0.75936	1.0219	3.9029

Figures

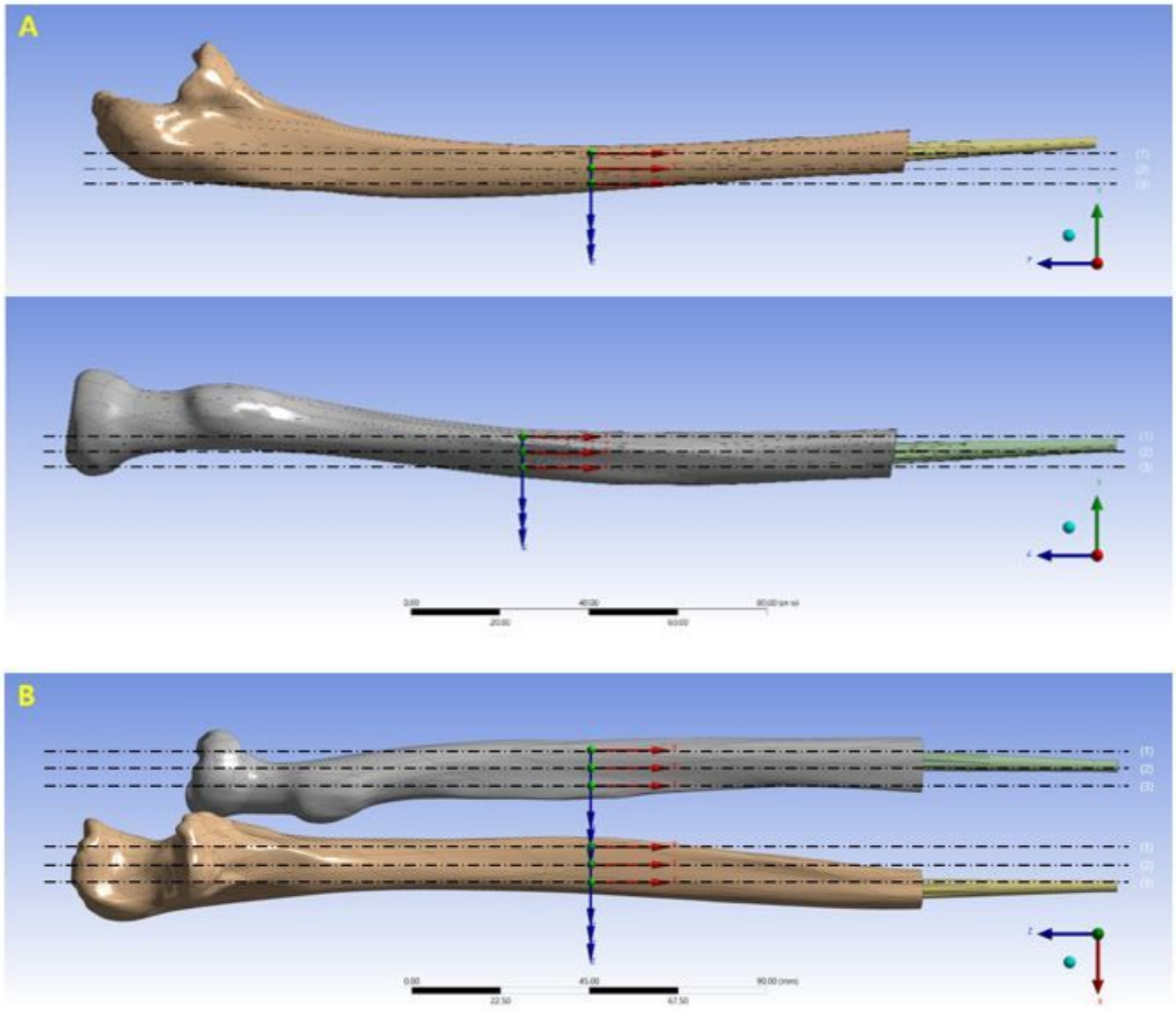

Figure 1

The stress distribution pattern and maximum equivalent stress were evaluated in each of the three sections(1, 2, 3) below; (A) X-axis and (B) Y and Z-axis.

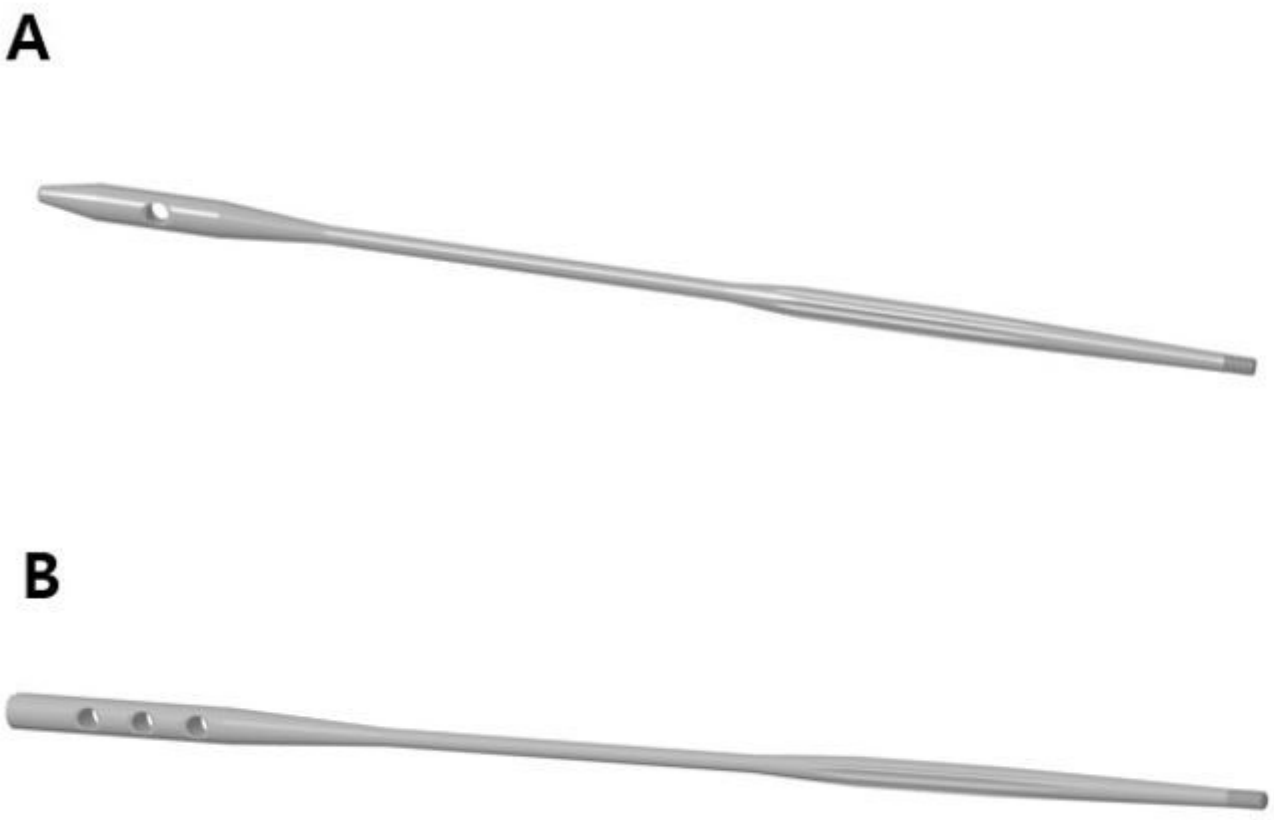

Figure 2

The new upper-extremity implant design assessed in this study. (A) Radius implant and (B) ulnar implant.

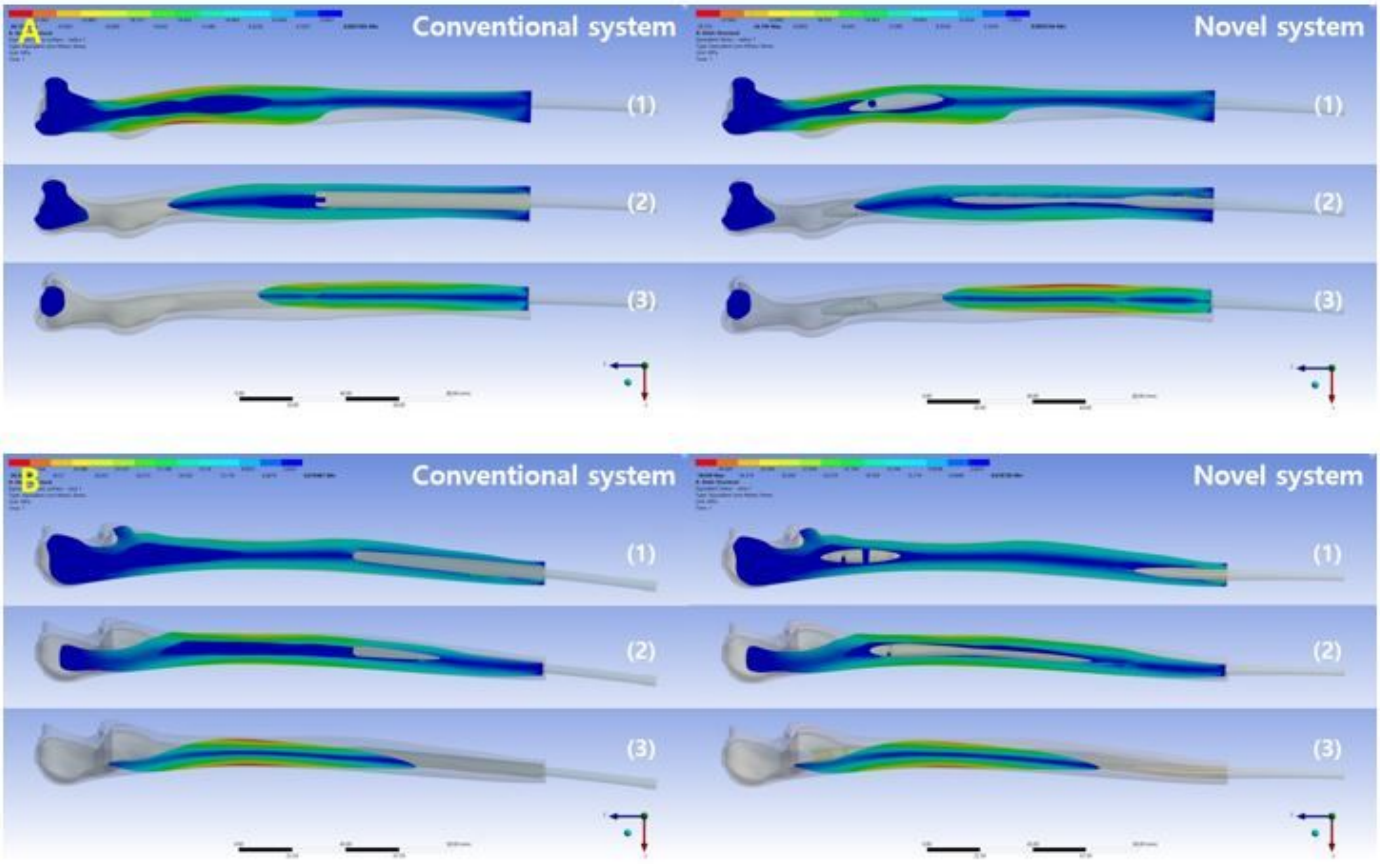

Figure 3

Stress distribution pattern when stress was loaded along the X-axis at the radius(A) and the ulna(B).

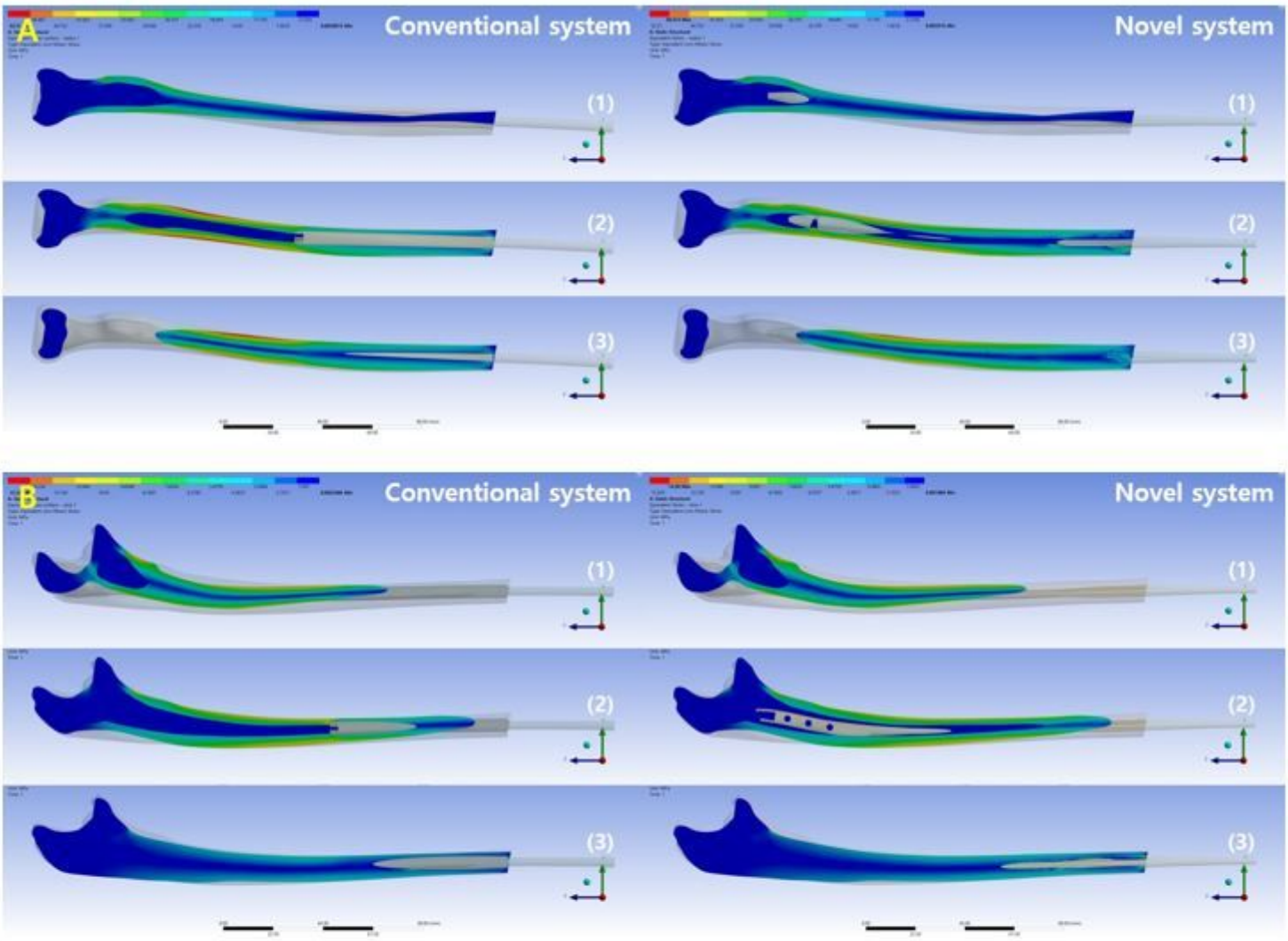

Figure 4

Stress distribution pattern when stress was loaded along the Y-axis at the radius(A) and the ulna(B).

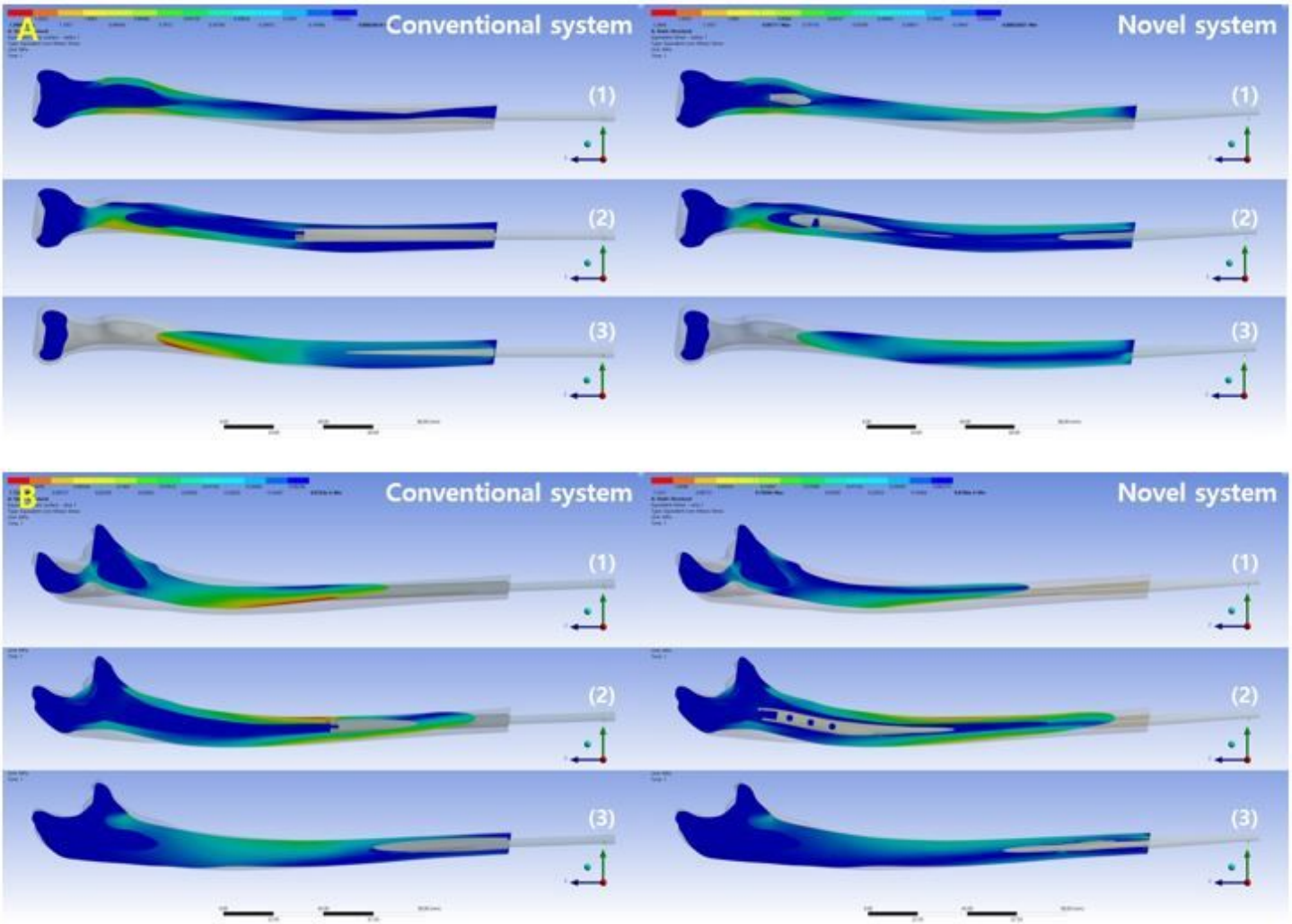

Figure 5

Stress distribution pattern when stress was loaded along the Z-axis at the radius(A) and the ulna(B).